

# Advanced Physical Models for Mask Data Verification and Impacts on Physical Layout Synthesis

Qi-De Qian\* and Sheldon X.-D. Tan†

\*IC Scope Research, Santa Clara, CA 95051

†Department of Electrical Engineering, University of California, Riverside, CA 92521  
qqian@icscope.com, stan@ee.ucr.edu

## Abstract

*The proliferation and acceptance of reticle enhancement technologies (RET) like optical proximity correction (OPC) and phase shift masking (PSM) have significantly increased the cost and complexity of sub-100 nm photomasks. The photomask layout is no longer an exact replica of the design layout. As a result, reliably verifying RET synthesis accuracy, structural integrity, and conformance to mask fabrication rules are crucial for the manufacture of nanometer regime VLSI designs. In this paper, we demonstrate a physical model based mask layout verification system. The new system consists of an efficient wafer-patterning simulator that is able to solve the process physical equations for optical imaging and resist development and hence can achieve high degree accuracy required by mask verification tasks. It is able to efficiently evaluate mask performance by simulating edge displacement errors between wafer image and the intended layout. We show the capabilities for hot spot detection, line width variation analysis, and process window prediction capabilities with a sample practical layout. We also discuss the potential of the new physical model simulator for improving circuit performance in physical layout synthesis.*

## 1. Introduction

The widespread acceptance of reticle enhancement technologies for sub 0.1 um integrated circuit manufacturing has dramatically complicated the mask data and increased the cost of advanced photomasks [1]. The increase in pattern complexity due to optical proximity correction, the tight requirements for critical dimension (CD) control, and the difficulties in defect inspection and repair all contribute to the manufacturing cost increase. For phase shift masks (PSM), the problems are compounded by additional requirements such as controlling the etching of multiple materials, alignment of multiple layers, and inspecting small defect with weak signals.

In addition to the added complexities in mask making, the growing array of reticle enhancement technologies (RET) also put more constraints on the physical layout design and verification as physical layouts must be RET-compliant and conform to the mask fabrication rules. For instance, the avoidance of phase conflicts in alternating PSM and generating OPC-friendly design layout are examples of those new constraints. Physical design and verification flow nowadays have to be overhauled to address various wafer and photomask manufacturing issues explicitly early in the design flow to achieve high-quality fabricated silicon at a reasonable point on the price-performance curve. It is encouraging to see increasing research efforts from industry and academia for this issue [8, 9, 10, and 12].

The complexities in mask data and manufacturing make it highly desirable to verify and optimize the mask data independently before committing to the costly fabrication process. An effective method for post-RET mask data verification is to simulate its image on the silicon wafer and compare it with the original design intent. This method places mask data in its intended operating environment and evaluate its performance metrics that have direct impact on wafer imaging. A simulation based verification system can evaluate the process window<sup>1</sup> for a product and give warning on certain performance limiting spots on the layout and thus significantly reduce the risk of mask data errors [2]. Once the troubling spots are identified, localized corrections can be applied to extend the process window in an intelligent way.

Existing model based mask layout verification systems have a few areas that requires further improvement. Firstly, they are typically implemented with the same simulation engine with model based OPC [2]. By sharing the simulation engine with OPC, the verification also inherits the errors of the OPC model. The logical dependency jeopardizes the probability of finding OPC errors, and reduces the reliability of the verification.

---

<sup>1</sup> A process window is the range of process parameter variations under which the line width remains within limits

Secondly, they employ empirical modeling approaches that cannot easily track acceptable variations in process conditions. In order to sample a different condition in the process window, a different set of models has to be developed, which consumes significant effort and time. In addition, there is no inherent reason why one set empirical models can judge the result of another if they are derived from the same set of mathematical formulation and training patterns.

In this paper, we propose to use a full-featured photolithography simulator for mask data verification. This type of simulators has been used extensively in lithography process development where they have demonstrated high accuracy for process predictions. Recently, we have developed fast algorithms to extend lithography simulator for large-scale mask data verification. We present a mask data verification flow around the physical lithography simulation core that is independent from the OPC engine, thus free from the logical dependency between OPC and its verification. The use of physical models opens the possibility for achieving higher prediction accuracy on complex layout configurations. In addition, physical model can naturally predict the pattern transfer behavior under process variations such as focus change. We will further discuss how physical layout design can efficiently leverage this physical model simulator to improve circuit performance and reduce the manufacturing variations.

## 2. Physical Model Based Mask Layout Verification Flow

Figure 1a shows the standard flow for reticle enhancement and optical proximity correction, with model based mask data verification block outlined with gray shading. Here we consider model based OPC as an independent module because it is also needed for all other reticle enhancement techniques as well as standard binary masks. The main manufacturing flow is shown on the left hand side. The design layout from a customer is modified with reticle enhancement, followed by model based OPC to produce a set of mask geometry data that is suitable for mask manufacturing. The model generation flow is shown on the right, where a test layout is printed with the same pattern transfer process to produce an experimental data set for empirical model fitting. The resulting model can then be used in the OPC engine to predict the wafer CD error. From that, the amount of mask correction can be calculated.

To implement physical model based mask data verification, one must calibrate the physical model by extracting the process parameters from the same data set used for empirical model fitting. The main task here is to

obtain resist-processing parameters such as development rate parameters and the post exposure bake diffusion length. The model can then be used in the mask layout verification (MLV) block to check the post-OPC mask data. The verification can be performed on the entire mask or, to save processing time, on sections of the mask that are most likely to have pattern transfer problems. In case such problems are found, the simulation pattern produced by the physical model and the corresponding mask section can be added to the data set for recalibrating the empirical model. This feed back system will gradually make the empirical model to become more predictive over time as more and more cases are added to the training set. At some point, the confidence level on the empirical model will reach a point when only occasional verification is needed in the full production mode.

Figure 1b shows the physical model based mask verification (PM-MLV) block in detail. The intended layout is derived from the design data by applying appropriate geometry operations such as scaling and sizing. This design intent is used as the standard for comparison. The other path of the verification process takes the mask layout as input and run through the wafer - patterning simulator. It simulates the wafer pattern by solving the equations describing image formation, resist exposure, post exposure bake, development and etching. The simulation parameters are set such that the resist and etching processes are accurately captured in the model. By doing so, any changes on the RET type, exposure tools settings, and thin film stack can be predicted by the physical simulator.

Fig. 1b shows the details of the MLV block. The output of the high accuracy wafer-patterning simulator is the outline of wafer image. The pattern differentiator in Fig. 1b compares this with the design intent and outputs the difference between the two patterns. The system characterizes the pattern difference by calculating the displacement of a line segment on the intended layout to its counterpart on the wafer image. Positive edge displacement indicates that the wafer pattern falls outside the original design polygon, and is larger than the design intent. Similarly, a negative edge displacement indicates that wafer pattern is smaller than the design intent. In order to better capture the variations along a polygon edge, the edges of the design intent polygons are subdivided into shorter segments for edge displacement calculation.

The subdivided edge segments are classified in a feature specific way in the data representing the design intent. For example, the segment located on a line end will carry a special flag indicating that line end pull back will be measured for this segment. Similarly, segments at long line edge may carry another flag indicating that transistor

gate or local interconnect variations will be measured at these segments. The feature specific classification flags help a user to impose different verification tolerance for each feature class of edges. By doing so, the verification process can be customized to better reflect the yield and performance of the product.

### 3. Hotspot Detection

Processing hotspots are the locations in the design where the magnitude of edge displacement is exceptionally large. Hotspots can form under a variety of conditions such as the original design being unfriendly to the RET that is applied to this chip, unanticipated pattern combinations in rule based OPC, or inaccuracies in model based OPC. When these hotspots fall on locations that is critical to the electrical performance of a device, they can reduce the yield and performance of the device.

Physical model based mask layout verification (PM-MLV) can identify the hot spots and subsequently repair them by applying physical model based OPC (PM-OPC) at these locations. We demonstrate this capability using the mask layout shown in Fig. 2a. The layout is for the poly gate layer with 90 nm target line width and dominating pitch of 300 nm. The cell size is approximately 11  $\mu\text{m}$  by 6.6  $\mu\text{m}$ . The mask layout is created by model based OPC using aerial image model only [4, 5]. After OPC, the standard deviation of edge displacement error is calculated to be 0.71 nm, which confirms that the wafer pattern as predicted by the aerial image simulation is in good agreement with the design intent.

The performance of this OPC mask created with simple aerial image model is verified using an optimized iso-focal<sup>2</sup> resist recipe that is a more realistic description of the patterning process. Fig. 2b shows the output of the pattern differentiator. The edge displacements are evaluated on 887 line segments on this cell. Our PM-MLV process discovers four segments with large edge displacement as shown in Fig. 2b. Interactive exploration shows that these points are located on either side of the short horizontal bars in “H” shaped patterns, as marked in Fig.2a. The standard deviation for edge displacement also increased 240% from 0.71 nm to 1.7 nm. This set of verification result shows that the mask data created by OPC with simple aerial image model would result in worse process and circuit performance than that suggested by the small correction residual.

---

<sup>2</sup> Iso-focal describes focus invariance of line width. Iso-focal can be optimized in such a way that the target line width is invariant under defocus

### 4. Proximity Induced Line Width Variation Statistics

Variations in line width due to lithography and etching often limit the performance of a circuit. The line width variation pattern changes as focus varies within allowed process control limits. Existing OPC methodology is aimed at reducing the line width variability at a nominal focus point, without considering the potential impact of focus change. In this case, physical model can be applied to obtain more complete and meaningful line width variation statistics by considering focus and other process parameter variations, the result of which can be used for performance optimization.

Fig. 3 shows the histogram for the edge displacement under defocus for a mask produced by physical model based OPC. At best focus, the mean edge displacement is zero, indicating an on-target CD distribution at 90 nm. The standard deviation of the edge displacement is 0.97 nm, which represents the residual of PM-OPC process. When this mask is printed under 0.15  $\mu\text{m}$  of defocus, the distribution broadens into a bi-modal form. We can clearly see the increase in the edge displacement envelope under defocus. The mean of the edge displacement, however, still stays at near zero, as in the best focus case. On average, the line width is not changed under defocus, as the number of edges with positive displacement roughly equals the number of edges with negative edge displacement. This behavior is consistent with the iso-focal process model we developed for this circuit.

On the other hand, if the same circuit layout is corrected with aerial image model and verified using aerial image model, a -14 nm average edge displacement will result with 0.15  $\mu\text{m}$  defocus. The range of variation also increases by nearly a factor of 7 from 0.71 to 3.5nm. The large difference in response between this and physical model based OPC and verification shows the strong influence of models on the OPC and verification results.

The edge displacement statistics produced by the physical model based OPC and verification process can be used in physical design flow to make ECAD tools manufacturability aware such that process variations can be reduced and circuit performance can be improved. We illustrated this concept in the following section.

### 5. Impacts on Physical Design Flows

The circuit design and mask processing are still basically separated from each other in current design and manufacturing flow. The design and process development team communicate only through a set of design rules. As we move into sub-100nm technologies, we have to

explicitly addressing various manufacturing issues early in the physical design flow to attain the best design performance, process window and uniformity in manufacture. A practical approach to considering this change in design-manufacturing interaction is through advanced process simulation that is transparent to circuit designers.

Fig. 4 shows a possible new mode of design-process interaction. For each new technology node, the equipment community publishes tool specifications early in the process development cycle. These parameters could be used to construct physical models well before an intended process becomes stable. These physical models can be applied early in the design phase to ensure that the layout can be optimized for the target processing technology. Manufacturing information such as process variations of channel lengths (channel edge displacement) and local interconnect variation under different RET configurations can be used to guide physical design to reach the best point on the performance-cost curve.

The key advantage of a physical model is that it does not depend on training patterns from a mature process. So it allows design library to be created in parallel with the process development. As a result, we can compute all the performance statistics like static/dynamic power consumption and delay for each OPC-processed cell in the library. We can pre-characterize OPC related information for each cell and use this information during placement to produce more OPC-friendly layouts. Specifically, we need to know how sensitive (*sensitive factor*) the critical dimensions (CDs) in a cell to its neighborhood patterns and how difficult to compensate the CDs in the cell. If an aggressive OPC is needed (like sub-resolution assistant features which may be outside of original cell layout), then the cell layout area has to be bloated. So we can build different *OPC configurations* for each cell in the library, each of them has different layout area and OPC performance in terms of statistic errors on CDs.

In the following, we show how different OPC configurations can affect the leakage power of a CMOS device. Static leakage power becomes a major concern for designers today, as it accounts for an increasing and significant portion of the total power budget in high-end microprocessors. This situation will become even worse with further reduction of threshold voltage ( $V_{th}$ ) of MOS devices. It was shown in [11] that CMOS device leakage currents  $I_{sub}$  varies exponentially with the change of channel length  $L$  as shown below:

$$I_{sub} = K(1/L) \exp(-CL),$$

where  $K$  and  $C$  are device dependent constants. As a result, the sub-threshold leakage currents are extremely sensitive to the channel length variations. It was shown in [11] that the mean leakage current of a chip under process variations can deviate significantly from the nominal leakage current in a typical 0.18  $\mu\text{m}$  COMS process. Following the same formula [11], we show how the mean leakage current and the standard deviation of a PMOS transistor vary with the changes of its channel lengths due to different OPC configurations. We use the process file from TSMC high-performance 0.13  $\mu\text{m}$  technology [13] for our sample calculation. Table 1 shows our calculated mean leakage and standard deviation of mean leakage of sub-threshold current of PMOS device under different OPC configurations.

**Table 1: Leakage current variation of PMOS device with variation of channel lengths.  $L=0.08\mu\text{m}$ ,  $W/L=5$ .**

OPC Cfg	Stdev. of L $\sigma$ (nm)	% Variation ( $3\sigma$ )	Mean $I_{sub}$ (nA)	Stdev. Of $I_{sub}$ (nA)
Phy-Model OPC	0.5	1.8%	4.0205	0.48
Std. OPC	2	7.5%	4.4661	1.88
No OPC	5	18.8%	6.9614	3.84

It can be shown that average leakage will significantly deviate from nominal value if no OPC is used. If OPC is employed, but is not optimized due to poor modeling or unexpected presence of neighborhood patterns, the average leakage will still %10 higher than the nominal value. With physical model based OPC and predictable neighborhood patterns, the channel length variation can be well controlled. As a result, the mean leakage current and its variation are reduced.

The statistical performance information of library cells can be leveraged during physical layout synthesis. For example, in the detailed placement phase, all the timing-critical or leakage cells (called *critical cells* in the sequel), which are also OPC sensitive, are instantiated with their best OPC configurations. Placement will legalize the added areas of those cells during refinement. If a cell is no longer a critical cell, its original layout will be used again. For OPC high sensitive critical cells, a fast on-line OPC process can be invoked to estimate the statistic errors for its neighborhood patterns. If the errors are still too large, some local cell swapping may be applied to get different neighborhood patterns or get more open area (adding dummy cells) around the critical cells or even re-synthesis the corresponding logics to make the resulting cell less OPC sensitive. This process is repeated until OPC CD errors on all the high sensitive critical cells are under control. Such cell-based OPC and the manufacturability-aware placement strategy bring many

advantages: First, it will improve the circuit performance and reduce the performance variations and thus unnecessary guardbanding, and lead to much more predictable circuit performances and manufacture yield. Second, with each layout pre-certified and OPC optimized by physical models, the final tape-out process would likely to be much simpler than the whole chip-wide, essentially flattened OPC and verification processes used today.

## 5. Conclusions

In this paper, we proposed a practical mask data verification flow in order to prevent data problems to propagate to the expensive mask making and wafer printing stage. Our new flow leverages the high accuracy of a wafer patterning simulator that predicts the wafer image by solving the equations that describe the physics and chemistry of the pattern transfer process. This system addresses the problems of the existing empirical model based OPC/RET flow and can be applied in parallel to improve the reliability and quality of the mask data. We show through a practical example that our system was capable of detecting and repairing wafer hot spots. We also discussed how edge displacement statistical information obtained from the new model simulator can be leveraged during physical synthesis flow to reduce the performance variations and improve the device manufacturability.

## References

- [1] Alfred Wong, "Resolution enhancement techniques in optical lithography", SPIE Oct. 2001
- [2] M. Rieger, L. Stirniman, "TCAD physical verification for reticle enhancement techniques", Solid State Technology Vol. 43, No 7, (134) 2000.
- [3] W. G. Oldham, S. N. Nandgaonkar, A. R. Neureuther, and M. O'Toole, "A general simulator for VLSI lithography and etching processes: Part I – application to projection lithography," IEEE Trans. Electron Devices ED-26, No. 4 (717) 1979.
- [4] C. A. Mack, "PROLITH: a comprehensive optical lithography model," Proc. SPIE Vol. 538 (207) 1985.
- [5] Qi-De Qian, F. A. Leon, "Fast Algorithms for 3D high NA lithography simulation", Proc. SPIE Vol. 2440 (372) 1995.
- [6] Chris A. Mack, Ching-Bo Juang, "Comparison of scalar and vector modeling of image formation in photoresist", Proc. SPIE Vol. 2440 (381) 1995.
- [7] A. Sekiguchi, M. Isono, and T. Matsuzawa, "Measurement of parameters for simulation of 193 nm lithography using Fourier transform Infrared baking system." Jpn. J. Appl. Phys. Vol 38 4936 1999
- [8] A.B. Kahng and Y.C. Pati, "Subwavelength optical lithography: challenges and impact on physical design", Proc. ACM intl. Symp. On Physical Design, pp.112—119, April 1999.

- [9] W. Grobman, M. Thompson, R. Wang, C. Yuan, R. Tian and E. Demircan, "Reticle Enhancement Technology: Implications and Challenges for Physical Design", Proc. ACM/IEEE 38<sup>th</sup> Design Automation Conference. pp.73-78, June 2001.
- [10] W. Maly, "Computer-aided design for VLSI circuit manufacturability", Proc. of IEEE, 78, pp.356—392, 1999.
- [11] A. Srivastava, R. Bai, D. Blaauw and D. Sylvester, "Modeling and analysis of leakage power considering within-die process variations", Proc. Intl. Symp. on Low Power Electronics and Design (ISLPE), pp.64—67, Aug. 2002.
- [12] F.M. Schellenberg, L. Capodiceci and B. Socha, "Adoption of OPC and the impact on design and layout", Proc. ACM/IEEE 38<sup>th</sup> Design Automation Conference. Pp.89 -- 92, June 2001.
- [13] TSMC 0.13um CMOS Process Technology: [http://www.tsmc.com/download/enliterature/013\\_bro\\_2002.pdf](http://www.tsmc.com/download/enliterature/013_bro_2002.pdf)

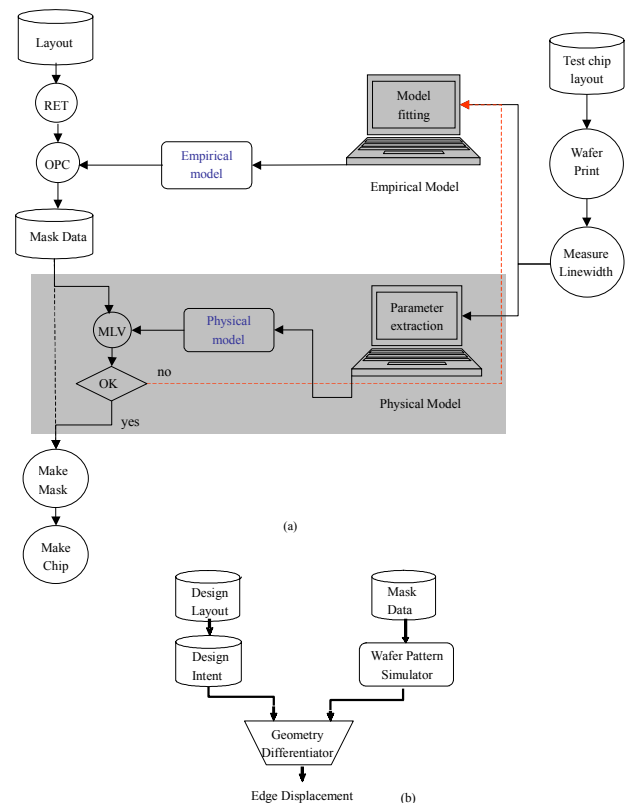


Fig. 1 (a) Model based optical proximity correction flow with verification block highlighted in gray shading. (b) Details of the MLV block where an independent, high accuracy wafer patterning simulator is used for verification. The geometry differentiator computes the difference between the intended layout polygons and the simulated pattern and output edge displacement values at locations of interest.

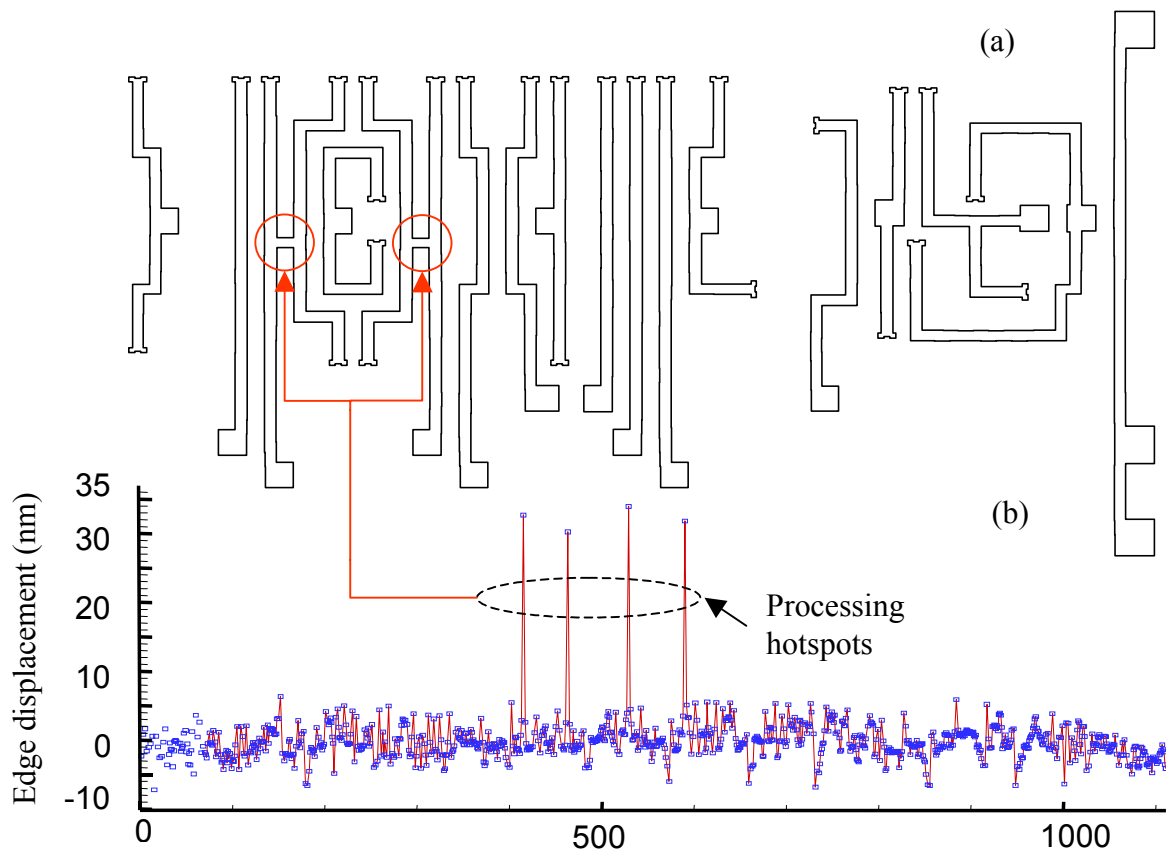


Fig. 2. Verification results for an OPC mask created with aerial image model. It revealed four processing hotspots where the edge displacements are much larger than elsewhere on this cell.

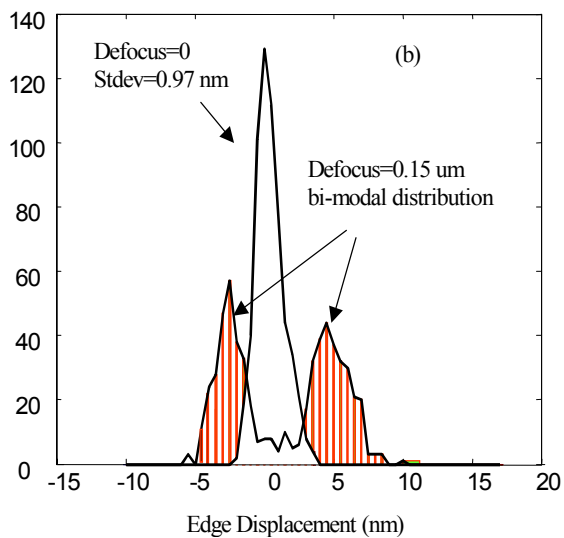


Fig. 3. Histogram of edge displacement error for a mask under gone PM-OPC with iso-focal resist model. The two peaks in the bi modal distribution are attributed to the nested and isolated edges respectively.

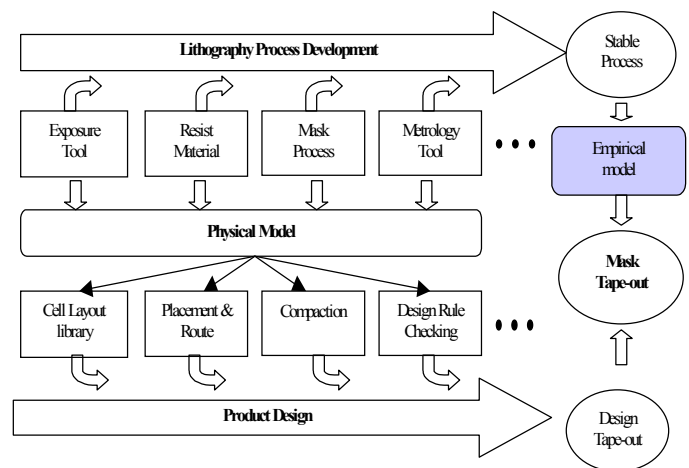


Fig. 4 New design and process flow. By communicating via physical models, one can optimize design and process concurrently.